ELSEVIER

Journal of Molecular Catalysis A: Chemical 163 (2000) 79–89

JOURNAL OF MOLECULAR CATALYSIS A: CHEMICAL

www.elsevier.com/locate/molcata

Nitric oxide interaction with Rh metal: kinetics of elemental steps and reaction with carbon monoxide

N. Kruse*

Chimie Physique des Surfaces et Catalyse Hétérogène, Universitè Libre de Brussels, Campus Plaine, CP 243, B-1050 Brussels, Belgium

Received 5 April 2000; accepted 10 July 2000

Dedicated to Prof. Michel Boudart on the occasion of his 75th birthday.

Abstract

Nitric oxide adsorption, thermal desorption and decomposition on a Rh model catalyst was studied using Pulsed Field Desorption Mass Spectrometry (PFDMS). This relaxation-type technique was applied as a chemical probe allowing the composition analysis in selected areas of about 200 atomic surface sites of the catalyst (with the latter being given in a nearly hemispherical morphology of a small tip). The kinetics of thermal desorption were addressed by varying the repetition frequency of the field pulses (usually between 100 kHz and 1 Hz) during the ongoing adsorption process at different temperatures between 450 K and 548 K. Assuming first order kinetics, the mean lifetimes $\bar{\tau}$ before thermal desorption of NO_{ad} were evaluated from the $(1 - 1/e)$ levels of the equilibrium coverages at long reaction times (i.e. low repetition frequencies). Evaluation in terms of an Arrhenius diagram led to $\bar{E}_d = 102$ kJ/mol for the activation energy and $\tau_o = 4 \times 10^{-14}$ s for the preexponential factor. The NO_{ad} dissociation kinetics were followed by monitoring as a function of time and at a constant pulse repetition frequency the buildup of surface nitrogen and oxygen. An activation energy $E_{dis} = 27$ kJ/mol was determined in this manner. A qualitative surface layer analysis was performed during the coadsorption and reaction of NO and CO and provide information on the formation of an isocyanate species, NCO_{ad}, at temperatures as high as 410 K.

Keywords: Nitric oxide; Rhodium; Isocyanides; Surface reactions; Thermal desorption kinetics

1. Introduction

The elucidation of the microscopic mechanisms and kinetics of the steady-state is still one of the major endeavours in heterogeneous catalysis. Ultimately, one would like to identify the individual steps and determine their rate parameters during the ongoing reaction. Once these data are available, the overall rate of a catalytic reaction can be computed so that predictions can be made by extrapolation to unknown conditions. Clearly, following such a procedure, recipes could be provided to develop new catalysts with improved activity and selectivity. In this or a similar way a surface scientist would describe his motivation to perform kinetic studies under well-defined reaction conditions. Historically, the kinetics of heterogeneous catalysis developed quite differently though. Important concepts have evolved on the basis of Bodenstein's steady-state approximation. As pointed out by M. Boudart [1,2], one of the Grand Seigneurs in the field, the identification of kinetically significant steps can help simplifying the reaction scheme so that "what we need to know in practice to

* Tel.: +32-2-6505710; fax: +32-2-6505708.
E-mail address: nkruse@ulb.ac.be (N. Kruse).

1381-1169/00/$ – see front matter
PII: S1381-1169(00)00401-5

develop, control, and improve solid catalysts, is much less what we want to know" [2]. One may add that what we want to know is not easily accessible and with this in mind the classical concepts are of as great an importance today as in the past.

It has been recognised early on that the combination of the steady-state analysis and in-situ transient studies provides a powerful means to address the detailed kinetics of catalytic reactions on solids [3]. The application of relaxation type methods which have been largely applied by Eigen [4] for studies in the liquid and the gas phase may be of particular interest. It has been shown [5] that such methods can be designed to monitor the course of a catalytic surface reaction with high spatial resolution allowing to specify the influence of various types of surface sites. Based on atom-probe field desorption originally invented by Müller et al. [6], the perturbation of the steady-state is achieved by field pulses and the kinetic analysis of the catalytic reaction is made by time-of-flight measurements of field desorbed species as a function of the pulse repetition frequency. Clearly, this technique can only be applied under model conditions of low gas pressures ($<10^{-3}$ mbar) and morphologically well-defined metal particle surfaces free of any non-conducting support material. In the present paper we shall make use of this technique to study the detailed kinetics of nitric oxide (NO) thermal desorption, decomposition and reaction with carbon monoxide (CO) on nearly hemispherical Rh single crystal particles. It will be demonstrated that kinetic data of these elemental steps are accessible in very dilute surface layers and that species can be identified that are hardly detectable with other techniques for reasons of insufficient sensitivity.

2. Experimental considerations

2.1. General

The experimental set-up is based on a combination of field ion microscopy (FIM) and time-of-flight field desorption mass spectrometry. Fig. 1 shows a typical field ion micrograph along with a ball model of the nearly spherical morphology of a Rh model catalyst called "field emitter tip". One can clearly recognise a number of different surface planes which usually exhibit different catalytic activity. During adsorption of gases the particle morphology frequently undergoes alterations. The FIM has been proven a powerful method to image these adsorbate-driven morphological features [7,8]. The atom-resolving capabilities of the FIM method can be extended to those of a local chemical probe of the catalyst surface. In this manner, a truly in-situ method is made available to identify adsorbed species and to establish surface reaction mechanisms and kinetics. The principle of operation of the so-called pulsed field desorption mass spectrometry (PFDMS) method is to produce high electric field strengths, $F < 50$ V/nm, in form of short negative field pulses (widths $\geq$100 ns, repetition rates $\leq$100 kHz) at an electrode in front of the catalyst particle. This causes field desorption of adsorbed species and the respective ions are subsequently mass-separated in a time-of-flight tube (Fig. 2). A probe-hole is mounted at the entrance of the flight tube. By tilting the tip sample in front of the hole, crystallographically different planes can be probed. The selection of a particular surface area is usually controlled in a separate experiment by field electron microscopy or FIM (Fig. 2). The size of the monitored area can be varied by means of an electrostatic lens located in the time-of-flight tube (not shown in the scheme). Usually, lens settings are used that allow areas with 150–250 atomic sites to be probed by field pulses. This size range can be taken as a compromise enabling still plane-specific measurements on the one hand and data acquisition with sufficient statistical significance on the other. This latter point is of considerable importance for studies of surface reaction kinetics.

Qualitative insight into the surface layer composition is obtained by using low-amplitude field pulses. Under these conditions, the layer composition is nearly constant throughout the measurements; small amounts removed by pulses are immediately refilled by adsorption between pulses. The identification of true surface species is not straightforward unless patterns of species fragmentation or association are known. Quite generally, assignments can be facilitated through temperature and pressure variation. However, the PFDMS method also allows to study the influence of the electric field strength through independent variation of the field pulse amplitude and the dc field. This procedure was applied by Kruse and Block [9] to reveal the field-induced formation of N_2O species

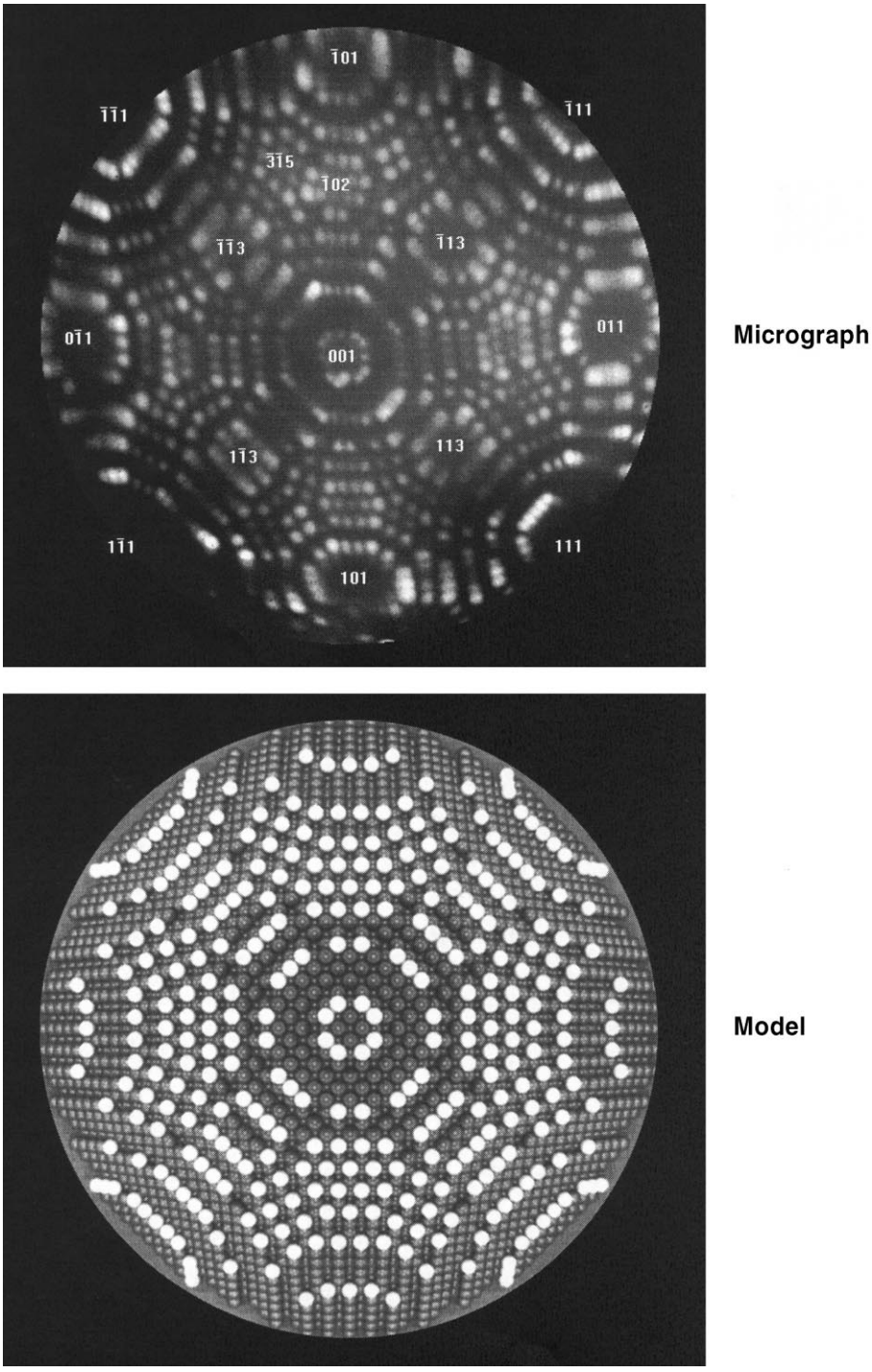

Fig. 1. Field ion micrograph (top) of a Rh tip (best image conditions in Ne at 35 V/nm, 55 K, radius of curvature: ~10 nm) along with a ball model (bottom).

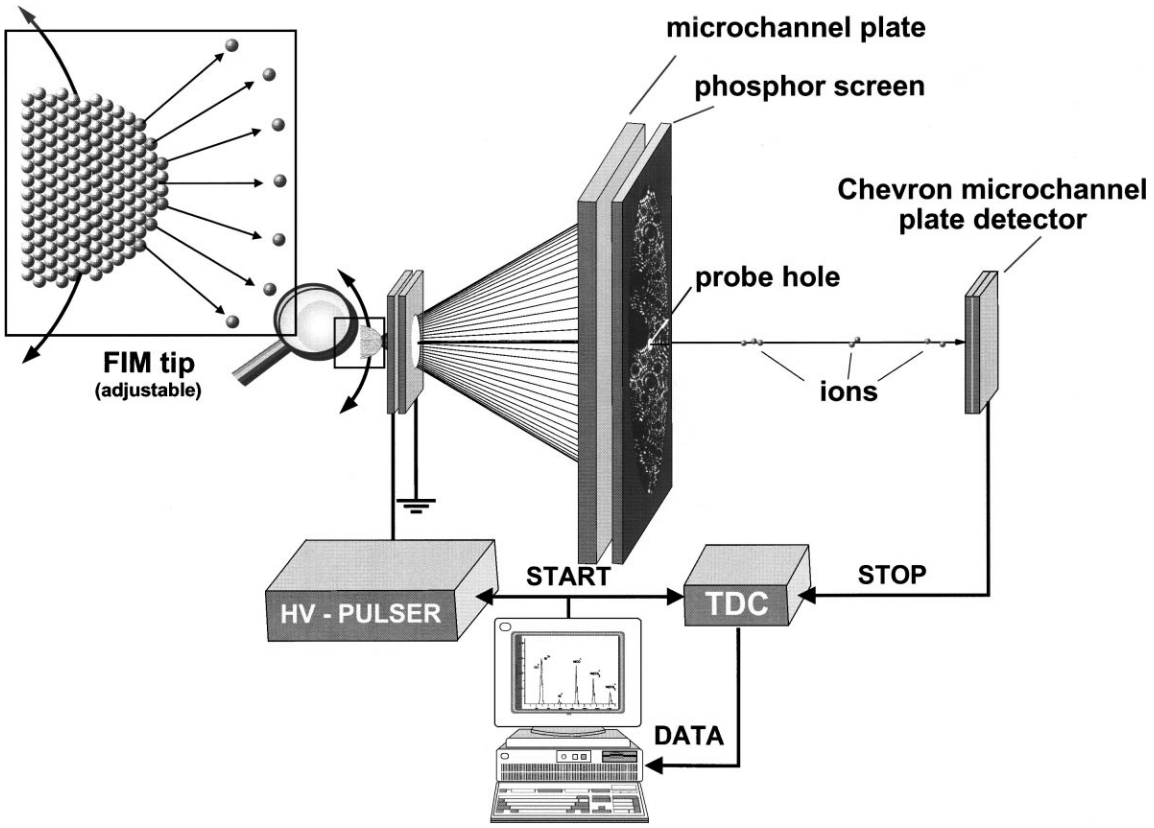

Fig. 2. Scheme of the PFDMS set-up: high-field pulses are applied to a counter electrode with a hole, located at 0.1 mm in front of the tip sample. A TDC (time-to-digital converter) is started synchronously and stopped by ions arriving on the detector at the end of a time-of-flight tube. A microchannel plate serves as image intensifier for field ion microcopy; a central hole selects a small area of the tip surface so that plane specific measurements can be performed.

during adsorption of NO on Pt tips. More recently, Madenach et al. [10] have demonstrated in a quantitative manner, how the binding energy of NO_{ad} on Rh is influenced by electric fields. Accordingly, the occupation of molecular orbitals is changed such that the metal–NO bond is weakened while the N–O bond is strengthened in the presence of a positive electric field.

Further details on the experimental set-up and on procedures applied to prepare tips can be found in the original literature [11].

2.2. Kinetic measurements

Kinetic data of surface processes can be obtained by varying the repetition rate, i.e. the reaction time t_R between the field pulses. This is usually done by scanning the range from 100 μs up to some seconds. For the measurements to be reported here no steady electric field (reaction field) was applied during t_R

In Fig. 3 the general experimental procedure for kinetic measurements is illustrated. Adsorption takes place field free, during t_R, by continuous impingement of gaseous NO. The field pulses stop the adsorption process and cause desorption of the adsorbed layer. Provided the layer removal is complete with each pulse, the ion intensity, i.e. the number of ions detected with each pulse (ions per pulse) is a measure of the surface coverage built up within the monitored area between any two pulses.

Three different pulse repetition rates, corresponding to short, medium, and long field free times t_R are depicted in Fig. 3. For short times as indicated on the

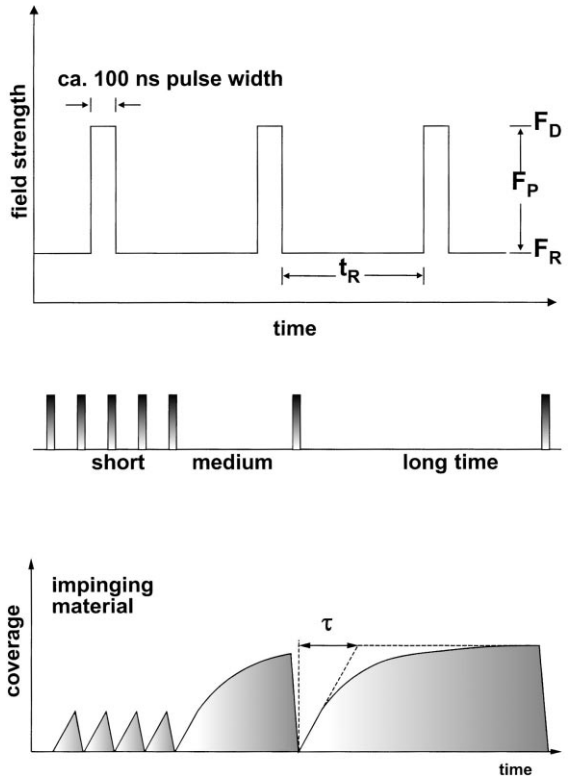

Fig. 3. Scheme illustrating field pulses of a certain repetition frequency; adsorption and reaction occur during the period t_R; a systematic variation of t_R provides kinetic information; F_D = total field strength; F_p = pulse field strength, F_R = steady field strength arbitrarily applied; in the present study $F_R = 0$.

left-hand side of the figure, the surface coverage that can be reached by adsorption during t_R is far below the monolayer limit. Only the initial stages of the adsorption process are monitored under these conditions. For long times and suitably chosen surface temperatures, substantial thermal desorption can take place between the pulses. In this case, only those molecules are field desorbed which have been adsorbed by, at most, their lifetime before the next pulse. Thus, the ion intensity and consequently, the concentration of the thermally equilibrated adsorbate do not increase any further. If the adsorption process is assumed to proceed with a constant sticking probability and thermal desorption to obey first order kinetics, $d\Theta/dt = -c/\tau$, the surface coverage follows a simple law

$$\Theta(t) = \Theta(\infty)(1 - e^{-t/\tau}) \quad (1)$$

where the relaxation time τ is the lifetime before thermal desorption, measured as the value of t_R at which the $(1 - 1/e)$ level of the equilibrium coverage $\Theta(\infty)$ is reached.

The temperature dependence of τ is parametrised via Frenkel's equation

$$\tau = \tau^0 e^{E/kT} \quad (2)$$

Both the activation energy E for thermal desorption and the preexponential τ^0 are accessible in this way.

3. Results

3.1. NO adsorption, thermal desorption and decomposition

The results to be presented here were obtained by probing ~150 atomic sites of the stepped surface region close to the (0 0 1) pole of the Rh sample. The surface was continuously dosed at a steady NO gas pressure of 1.3×10^{-5} Pa. Fig. 4 presents a typical time-of-flight mass spectrum obtained with a field strength $F_D = 28$ V/nm (pulses only, no steady reaction field) which turned out to be high enough to keep the surface dynamically clean. Under these conditions field evaporation of the substrate material takes place as evidenced by the occurrence of Rh^+ and Rh^{2+} ions.

As is clearly seen in Fig. 4, the mass spectrum is dominated by NO^+ ions. It is concluded that the surface layer contains mainly molecularly adsorbed NO at a reaction temperature of $T = 547$ K. The small amount of $RhNO^+$ ions possibly indicates field desorption of NO_{ad} from step sites with the simultaneous removal of a Rh step atom. The maximum NO_{ad} concentration built up during $t_R = 200\,\mu s$ is below 10^{-4} monolayer.

Moderate intensities are found for RhO^{2+}, RhN^{2+}, Rh_2N^{2+} and RhO^+. Also O^+, N^+ and $O_2{}^+$ ions are detected, however, for the experimental conditions underlying Fig. 4, their intensities are lower than those of the metal containing species. It is concluded that NO_{ad} undergoes partial dissociation during t_R, so that oxygen and nitrogen atoms are deposited on the surface. This result is in agreement with the catalytic behavior known for Rh metal. It is interesting that the products of NO_{ad} dissociation are almost exclusively field desorbed along with the removal of Rh atoms.

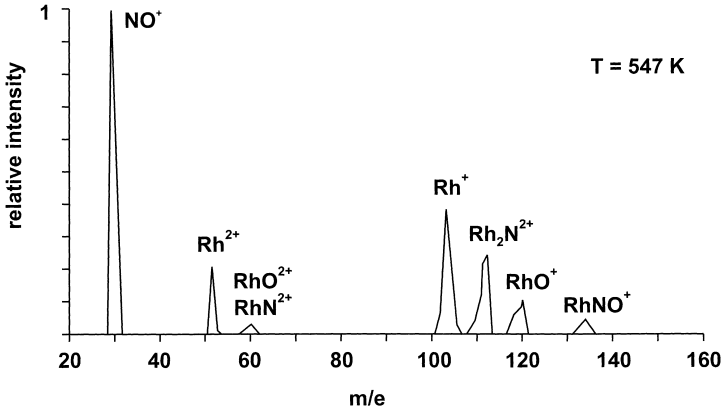

Fig. 4. Time-of-flight mass spectrum of NO on Rh (0 0 1) containing step sites; NO pressure: 1.3×10^{-5} Pa; desorption field $F_D \approx 28$ V/nm; no steady reaction field ($F_R = 0$); $T = 547$ K.

This process occurs most easily at steps because the local electric field is highest there. For more detailed considerations see [12].

We will now focus on the thermal desorption kinetics of NO_{ad}. For this purpose we followed the procedure described in the experimental part of the paper and varied the reaction time, t_R, from 100 μs to ~1 s at various temperatures between 450 and 548 K (Fig. 5). In order to ensure quantitative field desorption a field strength of 28 V/nm was used. Under these conditions, the intensities are a measure of the surface coverages built up during the reaction time t_R. About 200 atomic sites in the vicinity of the Rh (0 0 1) pole were probed by field pulses (no steady reaction field present) while dosing the sample continuously at $P_{NO} = 1.3 \times 10^{-5}$ Pa.

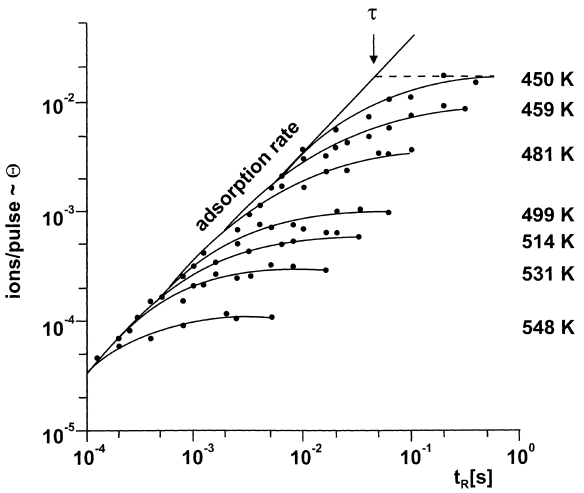

Fig. 5. Dependence of NO^+ ion intensity on tip temperature and reaction time t_R; monitored area: ~200 atomic sites, $P_{NO} = 1.3 \times 10^{-5}$ Pa; desorption field strength: 28 V/nm (only field pulses, no steady reaction field).

All curves in Fig. 5 show the same trend. At short times, t_R, the NO^+ ion intensities increase linearly with t_R. At long times (compared with the mean lifetime $\bar{\tau}$), the NO^+ intensities level off. Increasing surface temperatures cause the constant level parts to be reached earlier and to decrease. This behavior reflects thermal desorption occurring during t_R, thus limiting the amounts of material that can be accumulated on the surface. As long as t_R is short, adsorption from the gas phase predominates over thermal desorption. At long t_R (compared with $\bar{\tau}$), however, both processes counterbalance, thus establishing steady-state conditions.

Provided (i) adsorption occurs with a constant sticking probability and (ii) thermal desorption follows first-order kinetics, the mean lifetimes $\bar{\tau}$ before thermal desorption of NO_{ad} can be evaluated from the $(1 - 1/e)$ levels of the equilibrium intensities (coverages) at long times. Condition (i) is met, since the the adsorption rate (the slope $d\theta/dt$ in Fig. 5) is seen to be constant at short times (and independent on the surface temperature). Condition (ii) is most probably met, since NO desorbs from a molecular adsorption state at overall low population. According to Fig. 5, values of $\bar{\tau}$ are between 0.3 and 47 ms for temperatures in the range $T = 450$–548 K.

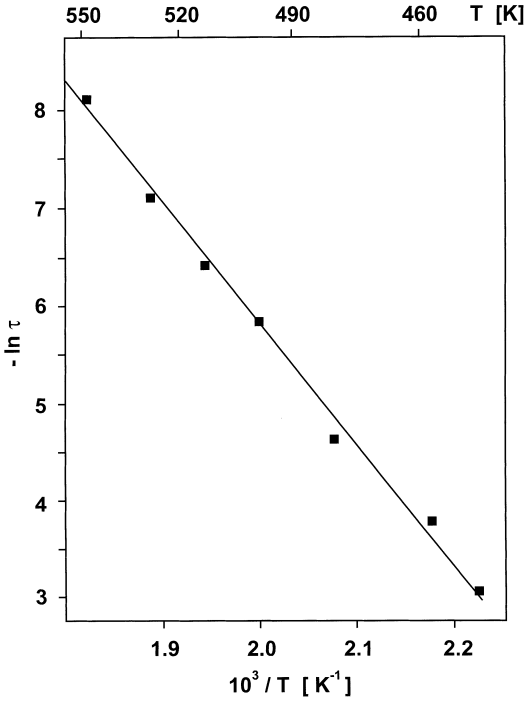

Fig. 6. Temperature dependence of the mean lifetimes τ of NO on a stepped Rh surface with (0 0 1) orientation of the terraces (Arrhenius plot of the data of Fig. 5); result: $\tau = 4 \times 10^{-14}\,\mathrm{s} \times \exp(102\,\mathrm{kJ/mol}/kT)$.

The temperature dependence of $\bar{\tau}$ can be evaluated by plotting $\ln\bar{\tau}$ vs. $1/T$ (Arrhenius diagram). According to Fig. 6, a straight-line dependence is obtained leading to an (apparent) activation energy $\bar{E}_\mathrm{d} = 102\,\mathrm{kJ/mol}$ (from the slope) and an (apparent) preexponential factor $\tau_0 = 4 \times 10^{-14}\,\mathrm{s}$ (from the intersect with the ordinate).

The Rh-oxide and -nitride ion intensities were also followed as a function of t_R. As a general result, these species exhibit a second order time dependence at short t_R. This finding is in agreement with a consecutive reaction model in which molecular NO adsorption occurs first and dissociation successively (i.e. $\Theta_{\mathrm{O,N}} \sim t_\mathrm{R}^2$ or $\ln\Theta \sim 2\ln t_\mathrm{R}$). At long times t_R, the slopes tend to decrease due to the occurrence of $\mathrm{NO_{ad}}$ thermal desorption. In order to avoid an overloading of Fig. 5, these data are not shown explicitly. Instead, we demonstrate that the NO dissociation kinetics can be alternatively addressed by measuring the temperature dependence of Rh-oxide and -nitride intensities. In Fig. 7, the $\mathrm{Rh_2N^{2+}}$ intensities are considered in detail (the respective $\mathrm{RhO^+}$ intensities behave in a similar manner, however, they are lower than those of $\mathrm{Rh_2N^{2+}}$). The measurements were performed under continuous gas supply at $P = 1.3 \times 10^{-4}$ Pa. The field strength, $F_\mathrm{D} = 30\,\mathrm{V/nm}$, is somewhat higher than adjusted previously (Fig. 5). About 150 atomic sites in the vicinity of the (0 0 1) pole of the Rh sample were probed. Temperatures were varied in the range between 300 and 570 K while keeping the reaction time at a constant value of $t_\mathrm{R} = 10\,\mathrm{ms}$.

Fig. 7 shows that the NO adsorbate is desorbed at high and constant rates up to $\cong$450 K (note that the respective intensities are plotted as number of ions per 10 s rather than as number of ions per pulse as in Fig. 5). Thus molecular adsorption is dominating for reaction times $t_\mathrm{R} = 10\,\mathrm{ms}$. A slight decrease of the ion rates at the highest temperatures indicates the transition into a steady-state condition which is maintained by continuous adsorption from the gas phase and thermal desorption during t_R. This feature is in complete agreement with the findings described in Fig. 5.

In contrast to $\mathrm{NO^+}$, the $\mathrm{Rh_2N^{2+}}$ intensities reveal a continuous increase with rising temperatures. Thus dissociative NO adsorption becomes increasingly important and competes with molecular adsorption at the high-temperature end in Fig. 7. The activation energy

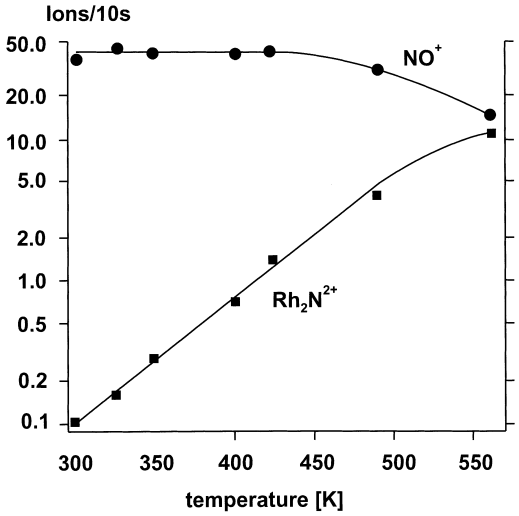

Fig. 7. Temperature dependence of $\mathrm{NO^+}$ and $\mathrm{Rh_2N^{2+}}$; monitored area ~150 atomic sites in the vicinity of the Rh (0 0 1) pole, $P_\mathrm{NO} = 1 \times 10^{-4}$ Pa, desorption field strength: 30 V/nm (only field pulses, no steady reaction field), $t_\mathrm{R} = 10\,\mathrm{ms}$.

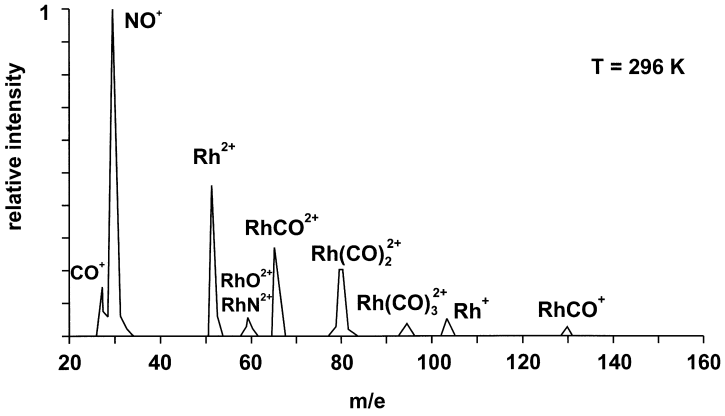

Fig. 8. Time-of-flight mass spectrum of a 1:1 mixture of NO/CO ($p_{tot} = 8.5 \times 10^{-5}$ Pa) on Rh (0 0 1) containing step sites; monitored area ~150 atomic sites; desorption field strength: $F_D \approx 26$ V/nm (field pulses only, no reaction field), $T = 296$ K, $t_R = 10$ ms.

for the NO dissociation process can be determined from the initial slope, d ln(l/*s*)/d*T* (at highest temperatures steady-state conditions seem to limit the extent of NO dissociation). A value $E_{dis} = 27$ kJ/mol is found which has to be compared with values of 8 kJ/mol obtained in measurements using a polycrystalline Rh foil [13] and 40 or 44 kJ/mol obtained in those using Rh single crystals of (1 1 1) [14] or (1 0 0) [15] symmetry.

3.2. NO and CO coadsorption and reaction

We finally demonstrate that the PFDMS method can also be used to study chemical reactions between different surface species. As an example we chose the NO–CO reaction and describe here qualitatively the various features occurring in the field desorption mass spectra.

Figs. 8 and 9 were obtained under identical experimental conditions, except for the reaction temperature which was adjusted to 296 K in Fig. 8 and to 410 K in Fig. 9. About 150 atomic sites in the vicinity of the (0 0 1) pole of the Rh sample (which is not the same as the one used in Figs. 5–7) were probed by pulses (no steady reaction field) of 26 V/nm after reaction intervals of $t_R = 10$ ms. A 1:1 mixture of NO and CO gas was continuously dosed to the surface at a total pressure of 8.5×10^{-5} Pa.

Fig. 8 contains the characteristic features known from adsorption of either gas alone. Accordingly, high intensities of NO^+ are found along with smaller

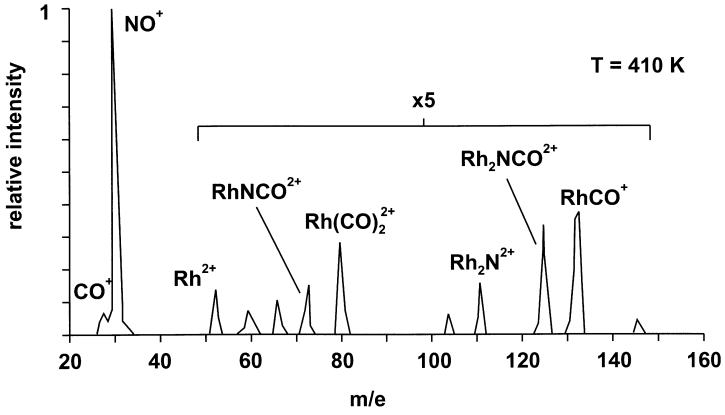

Fig. 9. Time-of-flight mass spectrum of a 1:1 mixture of NO/CO on Rh (0 0 1) containing step sites; same conditions as in Fig. 8, except for $T = 410$ K here.

ones of RhO^{2+} and RhN^{2+}. This behavior, similar to Fig. 4, demonstrates NO molecular adsorption to dominate over decomposition at 296 K in an NO/CO co-adsorbed layer. By contrast, only moderate intensities are found for CO^+ while those of $Rh(CO)_x{}^{2+}$ ($x = 1-3$) are somewhat higher. The occurrence of these latter species was previously analysed in detail and coherently interpreted as being due to the formation of adsorbed Rh-subcarbonyls [8].

In Fig. 9, obtained after increasing the temperature to 410 K, only the intensities of NO^+ are high while those of all other species are lower as compared to Fig. 8. Interestingly, however, $RhNCO^{2+}$ and Rh_2NCO^{2+} species are seen to occur in the high-temperature mass spectrum. This is interpreted as being due to the formation of adsorbed isocyanate, NCO_{ad}. We mention that these species disappear from the mass spectra as soon as a steady reaction field is switched on. This observation strengthens the argumentation that isocyanate is formed chemically according to $N_{ad} + CO_{ad} \rightarrow NCO_{ad}$. The detailed reaction kinetics must await further studies by reaction time variation.

4. Discussion

In this paper we have provided (i) kinetic data of the NO thermal desorption and decomposition on stepped Rh (0 0 1) and (ii) evidence for the formation of isocyanate species in an NO/CO co-adsorbed layer on the same surface. Some of the findings need further inspection and discussion.

One of the interesting features observed in part (i) is that molecular adsorption of NO dominates over dissociation up to the highest temperatures selected in this study ($T = 548$ K). This result also holds when probing the stepped surface region close to the (1 1 1) plane and is in contrast to most of the results obtained with macroscopic single crystal surfaces [14,16–19] which revealed complete dissociation of small NO_{ad} concentrations during heating from low temperatures to above 300 K. Both N_2 and O_2 (due to recombination reactions), rather than NO thermal desorption were observed in these studies. Obviously, NO_{ad} dissociation on Rh is a rather slow process which occurs to only a relatively small extent at a reaction time $t_R = 200\,\mu s$ underlying Fig. 4, but is complete in a TPD measurement with a time constant of the order of some tens of seconds.

The NO dissociation kinetics were measured by temperature variation at $t_R = 10$ ms. An activation energy $E_{dis} = 27$ kJ/mol was found. No information was gleaned for the preexponential factor, ν^0_{dis}, from these measurements. For comparison, Villarrubia and Ho [14] have reported on $E_{dis} = 44$ kJ/mol along with $\nu^0_{dis} = 10^{11.9\pm0.7}\,s^{-1}$ for NO dissociation on Rh (1 0 0). These data suggest fast rather than slow dissociation. Obviously, the preexponential factor plays an important role and can overcompensate the effect of a low activation energy. Quite interestingly, a strong compensation effect was found in studies of NO decomposition on Rh foils [13] and (1 1 0) single crystals [20]. For example, temperature-programmed static secondary ion mass spectrometry (TPSSIMS) on Rh (1 1 0) resulted in $E_{dis} = 15$ kJ/mol and $\nu^0_{dis} = 79\,s^{-1}$. In a subsequent study very similar data were found by Auger lineshape analysis [21]. Borg et al. [15], in a TPSSIMS study similar to ours, found $E_{dis} = 40 \pm$ kJ/mol and $\nu^0_{dis} = 10^{6\pm1}\,s^{-1}$ for NO dissociation on Rh (1 1 1) and considered these data effective rather than fundamental. The authors corrected their values to "more reasonable ones" by assuming an ensemble effect to be in operation. Despite some theoretical efforts [22] it seems that a realistic microscopic theory of the compensation effect is presently missing. Such a theory should also take into account the possibility of adsorbate-driven surface reconstruction which is known to occur on (0 1 1), (0 0 1) and other planes of Rh metal.

In turning to the kinetics of NO thermal desorption, we find reasonable agreement of our data, $\bar{E} = 102$ kJ/mol and $\tau_0 = 4 \times 10^{-14}$ s, with those reported in the literature for NO on Rh (1 0 0) [14,18,23]. For example, Villarrubia and Ho [14] determined $E_d = 118$ kJ/mol and $\tau_0 = 10^{-14}$ s by temperature programmed electron energy loss spectroscopy (TP-EELS) with varying heating rates and an initial surface coverage $\Theta_{NO} = 0.5$ monolayer which is much larger than the Θ values usually built up in our measurements. In PFDMS measurements at 450 K the maximum Θ_{NO} values remain below 10^{-2} monolayer under conditions of thermal equilibrium. Thus, it is safe to state that our rate data are not influenced by mutual interactions between species of the adsorbed layer.

According to the results presented in this paper it seems that step sites do not exert a strong influence on the NO thermal desorption kinetics. This is quite an interesting result in view of the different behavior observed for Pt metal. For example, PFDMS [11] and MBRS [24,25] (molecular beam relaxation spectroscopy) studies of NO thermal desorption have clearly demonstrated that steps on a Pt (1 1 1) surface act as trapping sites for adsorbed NO. Consequently, the measured lifetimes were found to be dominated by the binding energies of NO_{ad} in steps rather than in terraces. A quantitative treatment of the effect was given in [11].

Returning to NO dissociation on Rh metals, there is ample evidence that steps are more active in N–O bond breaking than terrace sites. Studies with macroscopic stepped single crystal surfaces [16,26] as well as with field emitter surfaces [27] clearly demonstrated the influence of steps. Hendrickx and Nieuwenhuys [27] provided an activity pattern of various planes and found the high index planes to decompose NO_{ad} most easily. In particular, Rh (3 2 1) and (3 2 2) exhibited the highest decomposition activity. Since our field desorption mass spectra contain mainly oxidic and nitride species in form of Rh-O(N) cluster ions, one is tempted to conclude on a dissociation process at steps. Such a conclusion, however, is not straightforward because nitrogen and oxygen atoms could alternatively form from NO_{ad} dissociation on terraces followed by diffusion to steps over distances of a few lattice sites only.

The field dependence of the NO decomposition on Rh was studied quite recently by Madenach et al. [10]. The authors report that for dc fields >5 V/nm N_2O formation occurs. A similar field effect was previously found for NO on stepped Pt (1 1 1) too [9]. Interestingly, the presence of a positive electric field changes, not only the reaction pathways but also influences the binding energies of NO_{ad}. A 15% reduction of the binding energy was found for NO on Rh (1 1 1) at 5 V/nm and is consistent with theoretical calculations [14]. The weakening of the M–NO bond in a positive field can be understood by assuming the electronic levels of the NO molecule to be raised relative to the metal band so that the sign of the electron transfer is partially reversed as compared to the field-free case. It is interesting to realise that N_2O formation cannot be observed merely with field pulses. Obviously, the time width of the pulses (some 100 ns) is not sufficient to open this pathway efficiently.

The formation of isocyanide species from NO and CO has long been considered to be characteristic for supported metal catalysts (see, for example, [28–30]). Moreover, there seems to be the general consensus that NCO_{ad} should be regarded as a spectator species rather than an active intermediate in the catalytic reduction to CO_2 and N_2. Following on the original work by Unland [31], the group of Solymosi has demonstrated that NCO species can be formed on Rh metal but are spilled-over to the support afterwards. In adsorption studies of HNCO on Rh (1 1 1), NCO_{ad} was found to form and to be stabilised by coadsorbed oxygen, with major amounts desorbing while heating to 390 K [32]. In the present study, clear evidence was obtained for a thermally activated NCO_{ad} formation in a surface layer containing CO, NO, O, N and $Rh(CO)_x$ species. The temperature range in which NCO_{ad} can be formed on a stepped Rh (0 0 1) surface still has to be studied in detail and so has the time dependence. We hope that the ultimate sensitivity of the PFDMS method will provide us insight into the reaction behaviour of mixtures of NO/CO which is not easily possible with other more conventional methods.

5. Conclusions

Pulsed field desorption mass spectrometry has been demonstrated to be a powerful technique capable of providing kinetic data of elemental steps occurring during catalytic reactions under model conditions. In comparing the results of NO interaction with Rh to those previously obtained with Pt, it becomes clear why Rh is the so much better deNO_x catalyst: there is not a single Rh crystal plane visited by our probe-hole technique which cannot break the N–O bond. Although the detailed kinetics of the dissociation process (the key step in deNO_x) are measurable under dilute conditions of very low surface coverages they remain obscure in the light of classical concepts such as transition state theory. Lacking a sound basis of understanding at this level it does not come as a surprise that attempts to extrapolate surface science-based simulations to high coverages of mutually interacting molecules failed so far. This is a clear

manifestation for the occurrence of a pressure-gap problem. The situation has been recently reviewed in detail for the NO reduction by CO [33] and seems to be much more involved than for CO oxidation with O_2 for which over many orders of magnitude of total pressure the kinetics and mechanisms are fairly well understood [34].

Acknowledgements

The author thanks the "Fonds National de la Recherche Scientifique" (No. 2.4516.98) and the "Communauté Française de Belgique" (ARC, No. 96/01-201) for financial support.

References

[1] M. Boudart, G. Djéga-Mariadassou, Kinetics of Heterogeneous Catalytic Reactions, Princeton University Press, Princeton, NJ, 1984.
[2] M. Boudart, in: G. Ertl, H. Knozinger, J. Weitkamp (Eds.), Handbook of Heterogeneous Catalysis, Wiley-VCH, 1997 (Chapters A1.1, A5.2).
[3] K. Tamaru, Adv. Catal. 15 (1964) 65.
[4] M. Eigen, Discuss Farad. Soc. 17 (1954) 194.
[5] J.H. Block, in: A.W. Czanderna (Ed.), Methods and Phenomena, Vol. 1, Elsevier, Amsterdam, 1975, p. 349.
[6] E.W. Müller, J.A. Panitz, S.B. McLane, Rev. Sci. Instrum. 39 (1968) 83.
[7] A. Gausmann, N. Kruse, Catal. Lett. 10 (1991) 310.
[8] N. Kruse, A. Gausmann, J. Catal. 144 (1993) 525.
[9] N. Kruse, J.H. Block, in: A. Crucq, A. Frennet (Eds.), Catalysis and Automotive Pollution Control I, Elsevier, Amsterdam 1987, p. 173.
[10] R.P. Madenach, G. Abend, H.J. Kreuzer, J.H. Block, Ber. Bunsenges Phys. Chem. 97 (1993) 353.
[11] N. Kruse, G. Abend, J.H. Block, J. Chem. Phys. 88 (2) (1988) 1307.
[12] N. Kruse, J. Vac. Sci. Technol. A8 (1990) 3432.
[13] C. Sellmer, V. Schmatloch, N. Kruse, Catal. Lett. 35 (1995) 165.
[14] J.S. Villarrubia, W. Ho, J. Chem. Phys. 87 (1987) 750.
[15] H.J. Borg, J.F.C.-J.M. Reijers, R.A. van Santen, J.W. Niemantsverdriet, J. Chem. Phys. 1010 (11) (1994) 10052.
[16] L.A. DeLouise, N. Winograd, Surf. Sci. 159 (1985) 199.
[17] T.W. Root, L.D. Schmidt, G.B. Fisher, Surf. Sci. 134 (1983) 30.
[18] P. Ho, J.M. White, Surf. Sci. 137 (1984) 103.
[19] L. Bugyi, F. Solymosi, Surf. Sci. 188 (1987) 475.
[20] V. Schmatloch, I. Jirka, N. Kruse, J. Chem. Phys. 100 (1994) 8471.
[21] G. Comelli, V.R. Dhanak, N. Pangher, G. Paolucci, M. Kiskinova, R. Rosei, Surf. Sci. 317 (1994) 117.
[22] H. Metiu, J.W. Gadzuk, J. Chem. Phys. 74 (1981) 2641.
[23] R.E. Hendershot, R.S. Hansen, J. Catal. 98 (1986) 150.
[24] T. Lin, G.A. Somorjai, Surf. Sci. 107 (1981) 573.
[25] C.T. Campbell, G. Ertl, J. Segner, Surf. Sci. 115 (1982) 309.
[26] D.G. Castner, G.A. Somorjai, Surf. Sci. 83 (1979) 60.
[27] H.A.C.M. Hendrickx, B.E. Nieuwenhuys, Surf. Sci. 175 (1986) 185.
[28] F. Solymosi, J. Sárkány, Appl. Surf. Sci. 3 (1979) 68.
[29] W.C. Hecker, A.T. Bell, J. Catal. 84 (1983) 200.
[30] W.C. Hecker, A.T. Bell, J. Catal. 85 (1984) 389.
[31] M.L. Unland, J. Catal. 31 (1973) 459.
[32] J. Kiss, F. Solymosi, Surf. Sci. 135 (1983) 243.
[33] V.P. Zhdanov, B. Kasemo, Surf. Sci. Rep. 29 (1997) 31.
[34] S.M. Landry, R.A. Dalla Betta, J.P. Lü, M. Boudart, J. Phys. Chem. 94 (1990) 1203.